RSC Advances

ROYAL SOCIETY OF CHEMISTRY

www.rsc.org/advances

Natural Nitric Oxide (NO) inhibitors from *Aristolochia mollissima*†

Zhen Dong,‡[a] Qiong Gu,‡[a] Bao Cheng,[b] Zhong-Bin Cheng,[a] Gui-Hua Tang,[a] Zhang-Hua Sun,[a] Jun-Sheng Zhang,[a] Jing-Mei Bao,[a] and Sheng Yin*[a]

Six new sesquiterpenoids, aristomollins A–F (**1**–**6**), and 24 known analogues (**7**–**30**) were isolated from leaves and stems of *Aristolochia mollissima*. Their structures were elucidated by spectroscopic analysis, and the absolute configurations of compounds **2–5** were determined by the chemical correlations and quantum chemical ECD calculations. Compound **1** represented an unprecedented 5,6-*seco*-4,5-cyclohumulane skeleton. All the compounds were examined for their inhibitory effects on the nitric oxide (NO) production induced by lipopolysaccharide (LPS) in BV-2 microglial cells, and compounds **4**, **9**, **28**, and **30** exhibited pronounced inhibition on NO production with IC_{50} values in the range of 5.7–9.9 μM, being more active than the positive control, quercetin (IC_{50} = 15.7 μM).

Introduction

Neuroinflammation has been considered as one of the pathological factors in neurodegenerative diseases including Alzheimer′s disease (AD), Parkinson′s disease (PD), stroke, dementia, and amyotrophic lateral sclerosis (ALS).[1,2] Activation of brain microglial cells and consequent overexpression of proinflammatory mediators such as nitric oxide (NO) are involved in the neuroinflammatory process. In addition, NO and superoxide lead to the formation of peroxynitrite, which results in numerous oxidation and potential destruction of host cellular constituents causing dysfunctional critical cellular processes, cell signaling pathway disruption, and brain cell death via cell apoptosis and necrosis.[3,4] There are numerous evidences suggesting that suppression of proinflammatory mediators (such as NO) and further inhibition of the neuroinflammatory responses in microglia could attenuate the severity or delay the progress of these neurodegenerative disorder.[5,6] Therefore, suppression of NO production in microglial cells might be an important and attractive therapeutic target for the treatment of neurodegenerative diseases.

Aristolochia mollissima Hance (Aristolochiaceae), a perennial shrub, is known as "Xun Gu Feng" in traditional Chinese medicine for its analgesic, anti-cancer, anti-rheumatic, and anti-inflammatory effects.[7] Previous investigations on this plant revealed a number of sesquiterpenes, aristolochic acids, and aristolactams, some of which exhibited anti-inflammatory,[8] antimicrobial,[9] and analgesic activities.[10] In our screening program aiming the discovery of natural NO inhibitors, the EtOAc fraction of the ethanolic extract of *A*. *mollissima* showed a certain inhibitory activity against the lipopolysaccharide (LPS)-induced NO production in BV-2 microglial cells. Subsequent chemical investigation led to the isolation of six new sesquiterpenoids (**1**–**6**), together with 24 known ones (**7–30**). Bioassay verified that compounds **3–5**, **9**, **17**, and **28–30** were responsible for the NO inhibitory activities of the EtOAc fraction, with IC_{50} values ranging from 5.7 to 29.8 μM. Herein, details of the isolation, structural elucidation, and NO inhibitory activities of these compounds are described.

Results and discussion

The air-dried powder of the leaves and stems of *A. mollissima* was extracted with 95% EtOH at room temperature (rt) to give a crude extract, which was suspended in H_2O and successively partitioned with EtOAc and *n*-BuOH. Various column chromatographic separations of the EtOAc extract afforded compounds **1–30**.

Compound **1**, a colorless oil, had a molecular formula $C_{15}H_{20}O$, as determined by HRESIMS ion at *m*/*z* 239.1401 $[M + Na]^+$ (calcd 239.1406). The IR absorption band at 1690 cm^{-1} indicated the presence of a carbonyl group. The ^1H NMR spectrum showed two olefinic methyl singlets [δ_H 1.81 (3H, H_3-14) and 1.44 (3H, H_3-15)], a terminal double bond [δ_H 5.15 (1H, s, H-5a) and 4.87 (1H, s, H-5b)], a formyl proton [δ_H 9.51 (H-1)], three olefinic protons [δ_H 7.21 (s, H-3), 5.14 (dd, J = 7.6, 7.6 Hz, H-7), and 4.85 (dd, J = 7.4, 7.4 Hz, H-11)], and a series of aliphatic methylene multiplets. The ^{13}C NMR spectrum, in combination with DEPT experiments, resolved 15 carbon resonances attributable to a highly conjugated aldehyde (δ_C 195.6), a terminal double bond (δ_C 112.0 and 146.4), three trisubstituted double bonds, two olefinic methyls, and four sp^3 methylenes. As five of the six degrees of unsaturation were consumed by four double bonds and a carbonyl group, the remaining degree of unsaturation required the presence of an additional ring. In the ^1H–^1H COSY spectrum two structural fragments **a** (C-7–C-8–C-9) and **b** (C-11–C-12–C-13) were first established by the correlations observed (Figure 2). The connectivities of the structural fragments **a**, **b**, the double bonds, the methyls and the formyl group were achieved by analysis of the HMBC correlations (Figure 2). In particular, HMBC correlations of H_3-14/C-4, C-6, and C-7, H_2-5/C-3, C-4, and C-6, and H-1/C-2, C-3, and C-13 incorporated Δ^2, Δ^4, and Δ^6 between C-7 and C-13. Moreover, HMBC correlations from H_3-15 to C-9, C-10, and C-11 further linked C-9 and C-11 via C-10 to afford an 11-membered macro ring. The geometry of Δ^6 was assigned as *Z* by NOESY correlation between H-7 and CH_3-14, while the geometries of Δ^2 and Δ^{10}

were both assigned as *E* by NOESY correlations of H-1/H-3 and H_2-12/CH_3-15, respectively. Thus, the structure of **1** was established as depicted and given the trivial name aristomollin A. Compound **1** featured an unprecedented 5,6-*seco*-4,5-cyclohumulane skeleton biogenetically related to co-isolated compounds **7** and **8**.

Compound **2**, a colorless oil, had a molecular formula $C_{15}H_{22}O_4$, as established by HRESIMS and ESIMS. The IR spectrum exhibited absorption bands for OH (3349 cm^{-1}) and lactone (1761 cm^{-1}) functionalities. The ^1H NMR spectrum showed two methyl singlets [δ_H 1.80 (3H, H_3-13) and 1.33 (3H, H_3-14)], a terminal double bond [δ_H 4.92 (2H, brs, H-12)], two protons bonded to carbons bearing heteroatoms [δ_H 5.35 (dd, J = 5.1, 2.9 Hz, H-6) and 4.03 (dd, J = 8.0, 6.6 Hz, H-1)], and a series of aliphatic methylene multiplets. The ^{13}C NMR spectrum, in combination with DEPT experiments, resolved 15 carbon resonances attributable to one carbonyl, a terminal double bond, two sp^3 quaternary carbons, four sp^3 methines (two bearing heteroatoms) four sp^3 methylenes, and two methyls. As two of the five degrees of unsaturation were accounted for a double bond and a carbonyl, the remaining three degrees of unsaturation required **2** to be tricyclic. The aforementioned information was in support of a eudesmane-type sesquiterpene with a lactone ring. Detailed 2D NMR analyses (^1H–^1H COSY, HSQC, and HMBC) permitted the establishment of the gross structure of **2** as depicted in Figure 2. The relative configuration of **2** was determined by analysis of the NOESY data and pyridine-induced solvent shifts. The *cis*-fused A/B ring system was established by the strong NOESY correlation of H-5/CH_3-14, which was supported by the diagnostic carbon chemical shift of CH_3-14 at δ_C 25.0, as the CH_3-14 in *trans*-eudesmanes usually resonated at around δ_C 14.0.[11–15] The NOESY correlations of H-5/H-6 and H-9α, H-9α/CH_3-13, H-1/H-8β, and CH_3-14/H-2α and H-3α indicated that the H-1, H-6, and the isopropenyl group were co-facial and arbitrarily assigned in α-orientation. As no convincing evidence was observed in the NOESY spectrum to assign the configuration of 4-OH, the ^1H NMR data of **2** was measured in $CDCl_3$ and C_5D_5N to obtain the pyridine-induced solvent shifts.[16,17] The solvent shifts of H-6 ($\Delta\delta_{CDCl_3 - C_5D_5N}$ = –0.35) and H-5 ($\Delta\delta_{CDCl_3 - C_5D_5N}$ = –0.34), indicating that the 4-OH/H-6 were 1,3-diaxial-oriented while 4-OH/H-5 were co-facial. Thus, 4-OH was assigned in α-orientation. The absolute configuration (AC)

of **2** was determined by comparing its experimental electronic circular dichroism (ECD) spectrum with those calculated by the Time-dependent density functional theory (TDDFT). In Figure **4**, the experimental ECD spectrum of **2** showed first negative and second positive Cotton effects at 230 nm and 192 nm, respectively, which matched the calculated ECD curve for **2a**, an isomer with a 1*R*, 4*R*, 5*S*, 6*R*, 7*R*, and 10*S* configuration, indicating that **2** possessed the same AC. Thus, compound **2** was assigned as depicted and named aristomollin B.

Compound **3**, a colorless oil, had a molecular formula $C_{15}H_{24}O_2$, as established by HRESIMS and ESIMS. The 1D NMR data of **3** were similar to those of aristoyunolin G (**9**)[18] except for the absence of signals for the formyl group and the presence of the signals for a hydroxymethyl group [δ_H 4.15 (1H, d, J = 14.1 Hz, H-14a) and 4.04 (1H, d, J = 14.1 Hz, H-14b); δ_C 67.6], indicating **3** was a formyl-reduced derivative of **9.** This was supported by the HMBC correlations of H-14/C-3, C-4 and C-5, H-3/C-14, and H-5/C-14 (Figure 2). The chemical transformation of **9** to **3** by $NaBH_4$ reduction further secured the structure of **3**. As the AC of **9** was assigned as 5*R*, 10*R*, and 12*R*, the AC of **3** was consequently determined as depicted. Compound **3** was given the trivial name aristomollin C.

Aristomollin D (**4**) was found to possess the molecular formula $C_{17}H_{24}O_3$ on the basis of HRESIMS data. The ^1H and ^{13}C NMR spectra of **4** showed high similarity to those of **9** except for the presence of an additional acetyl group signals [δ_H 1.99 (3H, s); δ_C 21.3 and 170.5], which indicated that **4** was an acetylated derivative of **9**. This was supported by the severely downfield-shifted H-12 signal in **4** with respect to that in **9** (δ_H 4.96 in **4**; δ_H 3.82 in **9**) and by the HMBC correlation from H-12 to the carbonyl group (δ_C 170.5). The AC of **4** was assigned to be the same as that of **9** based on the chemical transformation of **9** to **4** by acetylation.

The molecular formula of aristomollin E (**5**) was deduced as $C_{15}H_{24}O_2$ by HRESIMS data. Its 1D NMR spectra bore a resemblance to those of aristoyunolin H (**10**)[18] except for the absence of signals for the formyl group and the presence of a hydroxymethyl group [δ_H 4.13 (1H, d, J = 13.7 Hz, H-14a) and 4.06 (1H, d, J = 13.7 Hz, H-14b); δ_C 67.8], indicating **5** was a formyl-reduced derivative of **10**. This was

supported by the HMBC correlations of H-14/C-3, C-4 and C-5, H-3/C-14, and H-5/C-14. The AC of **5** was determined to be the same as that of **10** (5*S*, 10*S*, and 12*R*) on the basis of the chemical transformation of **10** to **5** by $NaBH_4$ reduction.

Compound **6** had a quasimolecular ion peak $[M + Na]^+$ at *m*/*z* 259.1663 in the HRESIMS, corresponding to the molecular formula $C_{15}H_{24}O_2$. The IR absorption bands at 3426 cm^{-1} and 1718 cm^{-1} showed the presence of the OH and carbonyl groups. The ^1H NMR spectrum showed three methyl singlets [δ_H 1.11 (H_3-15), 0.98 (H_3-12) 0.95 (H_3-13)], a formyl doublet [δ_H 9.54 (d, J = 3.0 Hz, H-14)], and a number of aliphatic protons. The 15 carbon resonances were classified by DEPT experiments as three methyls, four sp^3 methylenes, five sp^3 methines, two sp^3 quaternary carbons, and a formyl group. The above-mentioned information was very similar to that of **22**,[19] a aromadendrane sesquiterpenoid co-isolated in the current study, except for the presence of a formyl group [δ_H 9.54; δ_C 203.1] and a sp^3 methine (δ_C 60.3) in **6** instead of a tertiary methyl (δ_C 24.4) and an oxygenated quaternary carbon (δ_C 80.3) in **22**, indicating that **6** was a 4-dehydroxyl-14-oxidation derivative of **22**. The HMBC correlations from the formyl proton (H-14) to C-3, C-4, and C-5, from H-3 to C-14, and from H-5 to C-14 afforded the gross structure as depicted. The NOESY interactions of H-1 with H-4, H-6, H-9α, and CH_3-15 indicated that these protons were co-facial and arbitrarily assigned in α-orientation. The large coupling constant between H-5 and H-6 (J = 9.6 Hz) indicated a *trans*-relationship of these protons,[19] and therefore H-5 was assigned in β-orientation. The NOESY correlations of H-5/CH_3-13 and H-6/H-7 indicated the *cis*-cyclopropane moiety was β-oriented. Thus, compound **6** was deduced as depicted and named as aristomollin F.

The known compounds madolin W (**7**),[20] madolin H (**8**),[21] aristoyunnolin G (**9**),[18] aristoyunnolin H (**10**),[18] aristoyunnolin E (**11**),[22] madolin F (**12**),[21] aristolactone (**13**),[19] versicolactone B (**14**),[23] madolin U (**15**),[22] aristoyunnolin B (**16**),[22] (+)-isobicyclogermacrenal (**17**),[24] madolin K (**18**),[19] madolin T (**19**),[25] spathulenol (**20**),[26] 15-hydroxyspathulenol (**21**),[27] aromadendrane-4β,10β-diol (**22**),[19] (−)-alloaromadendrane-4β,10β-diol (**23**),[28] versicolactone C (**24**),[23] manshurolide (**25**),[29] aristoyunnolin F (**26**),[22] versicolactone D (**27**),[30] aristophyllide A (**28**),[31]

aristophyllide B (**29**),[31] and aristoloterpenate-I (**30**)[32] were identified by comparison of their NMR data with those in the literature.

Compounds **1**–**30** were evaluated for their inhibitory effects on the NO production in LPS-induced BV-2 microglial cells using the Griess assay.[5] Compounds **1**, **2**, **6**–**8**, **10**–**16**, and **18**–**27** were inactive (< 50% inhibition at 50 μM), while compounds **3**, **5**, **17**, and **29** showed moderate inhibitory activities with IC_{50} values ranging from 15.7–29.8 μM. Compounds **4**, **9**, **28**, and **30** showed remarkable inhibitory activities with IC_{50} values of 9.0, 9.9, 5.7, and 8.7 μM, respectively, more active than the positive control quercetin (IC_{50} = 15.7 μM), a well-known NO inhibitor (Table 3). The inhibitory curves of **4**, **28**, and quercetin were represented in Figure 5. To investigate whether the inhibitory activities of the active compounds were generated from their cytotoxicity, the effects of compounds **3–5**, **9**, **17**, and **28–30** on LPS-induced BV-2 microglial cell viability were measured using the MTT method. These eight compounds (up to 80 μM) did not show any significant cytotoxicity with LPS treatment for 24 h.

Conclusions

In summary, six new sesquiterpenoids and 24 known analogues were isolated from leaves and stems of *A. mollissima*. Their structures were elucidated by spectroscopic analysis, chemical correlations, and quantum chemical ECD calculations. Compound **1** represented an unprecedented 5,6-*seco*-4,5-cyclohumulane skeleton biogenetically related to the co-isolated cyclohumulane sesquiterpenoids, **7** and **8**. All the compounds were examined for their inhibitory effects on the nitric oxide (NO) production induced by lipopolysaccharide (LPS) in BV-2 microglial cells, and compounds **4**, **9**, **28**, and **30** exhibited pronounced inhibition on NO production with IC_{50} values in the range of 5.7–9.9 μM, being more active than the positive control, quercetin (IC_{50} = 15.7 μM). As the NO-suppression activity may attenuate the severity or delay the progress of neurodegenerative disorder, the evaluation of these active compounds on certain neurodegenerative diseases models, such as AD and PD, need

further exploration.

Experimental section

General experimental procedures

Optical rotations were measured on a Perkin-Elmer 341 polarimeter, and CD spectra were obtained on an Applied Photophysics Chirascan spectrometer. UV spectra were recorded on a Shimadzu UV-2450 spectrophotometer. IR spectra were determined on a Bruker Tensor 37 infrared spectrophotometer. NMR spectra were measured on a Bruker AM-400 spectrometer at 25 °C. ESIMS was measured on a Finnigan LCQ Deca instrument, and HRESIMS was performed on a Waters Micromass Q-TOF instrument. A Shimadzu LC-20 AT equipped with a SPD-M20A PDA detector was used for HPLC and a YMC-pack ODS-A column (250 × 10 mm, S-5 μm, 12 nm) were used for semi-preparative HPLC separation. Silica gel (300–400 mesh, Qingdao Haiyang Chemical Co., Ltd.), C_{18} reversed-phase silica gel (12 nm, S-50 μm, YMC Co., Ltd.), Sephadex LH-20 gel (Amersham Biosciences), and MCI gel (CHP20P, 75–150 μm, Mitsubishi Chemical Industries Ltd.) were used for column chromatography. All solvents used were of analytical grade (Guangzhou Chemical Reagents Company, Ltd.).

Plant material

Leaves and stems of *A. mollissima* were collected in March 2013 from Jiangxi Province, P. R. China, and were authenticated by Prof. You-Kai Xu of Xishuangbanna Tropical Botanical Garden, Chinese Academy of Sciences. A voucher specimen (accession number: XGF201303) has been deposited at the School of Pharmaceutical Sciences, Sun Yat-sen University.

Extraction and isolation

The air-dried powder of leaves and stems of *A. mollissima* (5.0 kg) was extracted with 95% EtOH (4 × 10 L) at rt to give a crude extract (382 g), which was suspended in H_2O (1.5 L) and successively partitioned with EtOAc (3 × 1.5 L) and *n*-BuOH (3 × 1.5 L). The EtOAc extract (175 g) was subjected to MCI gel

column chromatography (CC) eluted with a MeOH/H_2O gradient (1:9 → 10:0) to afford five fractions (I−V). Fr. I (5.6 g) was chromatographed over a C_{18} reversed-phase (RP-C_{18}) column eluted with MeOH/H_2O (5:5 → 10:0) to afford five fractions (Fr. Ia–Ie). Fr. Ia (1.1g) was separated on silica gel CC (PE/EtOAc, 6:1) to give **14** (150 mg). Fr. Ie (1.6 g) was separated on silica gel CC (PE/acetone, 3:1), followed by a Sephadex LH-20 column using ethanol as eluent to give **15** (22 mg), **16** (30 mg), **24** (15 mg), and **2** (7 mg). Fr. II (10.2 g) was subjected to silica gel CC (PE/EtOAc, 8:1 → 1:2) to give four fractions (Fr. IIa–IId). Fr. IIb (3.4 g) was purified on silica gel CC (PE/EtOAc, 5:1) to obtain **7** (50 mg), **18** (42 mg), and **6** (18 mg). Fr. IIc (0.9 g) was applied to silica gel CC (CH_2Cl_2/acetone, 25:1 → 5:1) to yield **9** (104 mg) and **10** (4 mg). Fr. IId (0.6 g) was chromatographed over a C_{18} reversed-phase (RP-C_{18}) column eluted with MeOH/H_2O (6:4 → 10:0) to afford **3** (7 mg) and **5** (15 mg). Fr. III (28 g) was subjected to silica gel CC (PE/EtOAc, 5:1 → 1:1) to give ten fractions (Fr. IIIa–IIIj). Fr. IIIc (1.9 g) was subjected to a RP-C_{18} silica gel CC (MeOH/H_2O, 6:4 → 10:0), followed by a silica gel CC (PE/acetone, 20:1 → 1:1) to afford **19** (50 mg), **20** (122 mg), and **25** (35 mg). Fr. IIIe (230 mg) was chromatographed over silica gel CC (CH_2Cl_2/MeOH, 200:1) to yield **12** (3 mg). Fr. IV (44 g) was chromatographed over an MCI gel column eluted with a gradient of MeOH/H_2O (6:4 → 10:0) to give eight fractions (Fr. IVa–IVh). Fr. IVa (2.3 g) was separated over RP-C_{18} CC using a gradient of MeOH/H_2O (6:4 → 10:0) to yield **17** (300 mg) and **1** (22 mg). Fr. IVb (8.8 g) was subjected successively to a silica gel CC (PE/EtOAc, 60:1 → 5:1), a RP-18 silica gel CC (MeOH/H_2O, 7:3 → 10:0), and a Sephadex LH-20 column (EtOH) to yield **8** (40 mg), **13** (1.2 g), **21** (15 mg), **11** (12 mg), and **22** (6 mg). Fr. IVc (2.7 g) was applied to silica gel CC (PE/EtOAc, 40:1 → 1:1) to give Fr. IVc1–IVc3. Fr. IVc1 (840 mg) was separated on a silica gel CC (PE/EtOAc, 50:1 → 30:1) to give **26** (7.1 mg) and **27** (15 mg). Further purification of Fr IVc2 (1.1 g) by silica gel CC (PE /$CHCl_3$, 4:1) afforded **4** (10.2 mg), **28** (10 mg), and **23** (4 mg). Fr IVc3 (600mg) was separated over RP-C_{18} CC using a gradient of MeOH/H_2O (7:3 → 10:0) to yield

29 (5.3 mg) and **30** (5 mg).The purity of compounds **1**–**30** was greater than 95% as determined by ^{1}H NMR spectra (Electronic Supplementary Information).

Aristomollin A (1). colorless oil; UV (MeOH) λ_{max} (log ε) 228 (3.99) nm; IR (KBr) ν_{max} 2923, 2853, 1690, 1459, 1377, 1219, and 1125 cm^{-1}; ^{1}H and ^{13}C NMR data, see Tables 1 and 2; positive ESIMS *m*/*z* 217.2 $[M + H]^+$; HRESIMS *m*/*z* 239.1401 $[M + Na]^+$ (calcd for $C_{15}H_{20}ONa$, 239.1406).

Aristomollin B (2). colorless oil; $[\alpha]^{20}_D$ +77 (*c* 0.23, $CHCl_3$); IR (KBr) ν_{max} 3349, 2934, 2865, 1761, 1453, 1218, and 1044 cm^{-1}; ^{1}H and ^{13}C NMR data, see Tables 1 and 2; positive ESIMS *m*/*z* 289.1 $[M + Na]^+$; HRESIMS *m*/*z* 289.1418 $[M + Na]^+$ (calcd for $C_{15}H_{22}O_4Na$, 289.1416).

Aristomollin C (3). colorless oil; $[\alpha]^{20}_D$ +210 (*c* 0.14, $CHCl_3$); IR (KBr) ν_{max} 3377, 2964, 2924, 2865, 1642, 1059, and 912 cm^{-1}; ^{1}H and ^{13}C NMR data, see Tables 1 and 2; positive ESIMS *m*/*z* 219.2 $[M - H_2O + H]^+$; negative ESIMS *m*/*z* 235.1 $[M - H]^-$; HRESIMS *m*/*z* 259.1668 $[M + Na]^+$ (calcd for $C_{15}H_{24}O_2Na$, 259.1669).

Aristomollin D (4). colorless oil; $[\alpha]^{20}_D$ +180 (*c* 0.28, $CHCl_3$); IR (KBr) ν_{max} 3495, 2925, 1735, 1694, 1456, 1370, and 1244 cm^{-1}; ^{1}H and ^{13}C NMR data, see Tables 1 and 2; positive ESIMS *m*/*z* 217.2 $[M - HOAc + H]^+$; HRESIMS *m*/*z* 299.1632 $[M + Na]^+$ (calcd for $C_{17}H_{24}O_3Na$, 299.1623).

Aristomollin E (5). colorless oil; $[\alpha]^{20}_D$ –247 (*c* 0.22, $CHCl_3$); IR (KBr) ν_{max} 3335, 2963, 2924, 2865, 1641, 1060, and 911 cm^{-1}; ^{1}H and ^{13}C NMR data, see Tables 1 and 2; positive ESIMS *m*/*z* 219.2 $[M– H_2O + H]^+$; negative ESIMS *m*/*z* 235.2 $[M - H]^-$; HRESIMS *m*/*z* 259.1669 $[M + Na]^+$ (calcd for $C_{15}H_{24}O_2Na$, 259.1669).

Aristomollin F (6). colorless oil; $[\alpha]^{20}_D$ –26 (*c* 0.33, $CHCl_3$); IR (KBr) ν_{max} 3426, 2928, 2867, 2718, 1718, 1455, 1376, and 1119 cm^{-1}; ^{1}H and ^{13}C NMR data, see

Tables 1 and 2; positive ESIMS *m/z* 219.2 $[M - H_2O + H]^+$; negative ESIMS *m/z* 235.3 $[M - H]^-$; HRESIMS *m/z* 259.1663 $[M + Na]^+$ (calcd for $C_{15}H_{24}O_2Na$, 259.1669).

ECD Calculation of 2a.

In general, conformational analyses were carried out via Monte Carlo searching using molecular mechanism with MMFF94 force field in the SPARTAN 04[33] software package. The results showed 4 lowest energy conformers for **2a** whose relative energy within 2.0 kcal/mol. Subsequently, the conformers were reoptimized using DFT at the B3LYP/6-31+G (d) level in gas phase in the GAUSSIAN 09 program.[34] The B3LYP/6-31+G (d) harmonic vibrational frequencies were also calculated to confirm their stability. The energies, oscillator strengths, and rotational strengths (velocity) of the first 60 electronic excitations were calculated using the TDDFT methodology at the B3LYP/6-311++G (2d, 2p) level in vacuum. The ECD spectra were simulated by the overlapping Gaussian function (half the bandwidth at 1/e peak height, σ = 0.6 eV).[35] For **2a**, the first 5 electronic excitations were adopted. To get the overall spectra, the simulated spectra of the lowest energy conformers were averaged according to the Boltzmann distribution theory and their relative Gibbs free energy (ΔG) (more details see Supplementary Information). Theoretical ECD spectrum of the corresponding enantiomer of **2a** were obtained by directly inverse the ECD spectra of **2a**.

Chemical transformation of 9 to 3.

$NaBH_4$ (1 mg) was added to a stirred solution of **9** (2 mg) in MeOH (0.5 mL), and the reaction was stirred at rt for 15 min. The mixture was then purified on Sephadex LH-20 (EtOH) to afford **3** (1.4 mg)**.** Compound **3** was identified by the ^{1}H NMR spectrum, MS data, and specific rotation.

Chemical transformation of 9 to 4.

Acetic anhydride (200 μL) was added to a stirred solution of **9** (2 mg) in freshly distilled pyridine (1 mL). The reaction was stirred at rt for 10 h and quenched by

adding 0.4 mL of H_2O. After removal of solvent under vacuum, the residue was purified on a flash silica gel column eluting with $CHCl_3$ to afford **4** (1.9 mg), which was identified by the ^1H NMR spectrum, MS data, and specific rotation.

Chemical transformation of 10 to 5.

To a stirred solution of **10** (2 mg) in MeOH (0.5 mL) was added $NaBH_4$ (1 mg). The mixture was stirred at rt for 15 min, and then was subjected to Sephadex LH-20 (EtOH) column to obtain **5** (1.5 mg). Compound **5** was identified by the ^1H NMR spectrum, MS data, and specific rotation.

Cell culture and viability assay.

BV-2 microglial cells were obtained from Southern Medical University (SMU) Cell Bank (Guangzhou, People's Republic of China). Cells were plated into a 96-well plate (2×10^4 cells/well). After 24 h, they were pretreated with samples for 30 min and stimulated with 1 μg/mL LPS for another 24 h. The cell viability of the cultured cells was assessed by MTT assay. Briefly, BV-2 cells were incubated with 200 μL MTT solution (0.5 mg/mL in medium) for 4 h at 37 °C, and then the supernatants were removed and residues were dissolved in 200 μL DMSO. The absorbance was detected at 570 nm using a microplate reader (Molecular Devices, USA) and analyzed using a SoftMax Pro 5 software (Molecular Devices, USA).

Measurement of NO production.

The NO concentration was measured by the Griess reaction. Briefly, BV-2 cells were treated with LPS (1.0 μg/mL) and compounds for 24 h. After that, 100 μL of culture supernatant was allowed to react with 100 μL of Griess reagent (1% sulfanilamide, 0.1% N-1-naphthylethylenediamine dihydrochloride in 5% phosphoric acid) for 10 min at rt in the dark. Then, the optical density (100 μL per well) was measured at 540 nm using a microplate reader (Molecular Devices, USA). Sodium nitrite was used as a standard to calculate the nitrite concentration. Inhibition (%) = $(1 - (A_{LPS+sample} - A_{untreated})/(A_{LPS} - A_{untreated})) \times 100$. The experiments were performed in triplicates,

and the data are expressed as the mean ± standard deviation (SD) values. Quercetin was used as a positive control.

[a]*Guangdong Provincial Key Laboratory of New Drug Design and Evaluation*, *School of Pharmaceutical Sciences, Sun Yat-sen University, Guangzhou, Guangdong 510006, P. R. China E-mail: yinsh2@mail.sysu.edu.cn; Fax: +86-20-39943090; Tel: +86-20-39943090*.

[b]*Institute of Chinese Medical Sciences, Guangdong Pharmaceutical University, Guangzhou, Guangdong 510006, P. R. China*

† Electronic supplementary information (ESI) available: 1D and 2D NMR spectra of **1**−**6**, ^{1}H NMR spectra of known compounds (**7**–**30**). Detail information for ECD calculation.

‡ These authors have contributed equally to this work.

Acknowledgments

The authors thank the National Natural Science Foundation of China (No. 81102339) and the Opening Project of Guangdong Provincial Key Laboratory of New Drug Design and Evaluation (2011A060901014) for providing financial support to this work.

Notes and references

1 D. Luo, T. C. T. Or, C. L. H. Yang and A. S. Y. Lau, *ACS Chem. Neurosci.*, 2014, **5**, 855–866.

2 S. D. Skaper, P. Giusti and L. Facci, *FASEB J.*, 2012, **26**, 3103–3117.

3 P. Wang and J. L. Zweier, *J. Biol. Chem.*, 1996, **271**, 29223–29230.

4 R. Radi, A. Cassina and R. Hodara, *Biol. Chem.*, 2002, **383**, 401–409.

5 J. Li, K. W. Zeng, S. P. Shi, Y. Jiang and P. F. Tu, *Fitoterapia*, 2012, **83**, 896–900.

6 B. Liu and J. S. Hong, *J. Pharmacol. Exp. Ther.*, 2003, **304**, 1–7.

7 T. S. Wu, A. G. Damu, C. R. Su and P. C. Kuo, *Nat. Prod. Rep.*, 2004, **21**, 594–624.

8 G. X. Li, D. H.Wang and Q. Liu, *Chin J Chin Mater Med.*, 1985, **10**, 39–41.

9 J. Q. Yu, Z. X. Liao, X. Q. Cai, J. C. Lei and G. L. Zou, *Environ. Toxicol. Pharmacol.*, 2007, **23**, 162–167.

10 Y. M. Chen, L. N. Wang, C. Cui, J. Y. Ma, W. W. Wang, Z. X. Li, J. Gong and S. F. Ni, *Anhui Nongye Kexue.*, 2013, **41**, 4322–4323.

11 Z. H. Cheng, T. Wu, S. W. A. Bligh, A. Bashall and B. Y. Yu, *J. Nat. Prod.*, 2004, **67**, 1761–1763.

12 A. Garcia and G. Delgado, *J. Nat. Prod.*, 2006, **69**, 1618–1621.

13 Z. Sun, B. Chen, S. Zhang and C. Hu, *J. Nat. Prod.*, 2004, **67**, 1975–1979.

14 N. Li, J. J. Chen and J. Zhou, *J. Asian Nat. Prod. Res.*, 2005, **7**, 279–282.

15 J. Kitajima, K. Kimizuka and Y. Tanaka, *Chem. Pharm. Bull.*, 2000, **48**, 77–80.

16 P. V. Demarco, E. Farkas, D. Doddrell, B. L. Mylari and E. Wenkert, *J. Am. Chem. Soc*., 1968, **90**, 5480-5486.

17 B. N. Su, R. Misico, E. J. Park, B. D. Santarsiero, A. D. Mesecar, H. H. S. Fong, J. M. Pezzuto and A. D. Kinghorn, *Tetrahedron*, 2002, **58**, 3453-3466.

18 R. B. Wu, Z. B. Cheng, Q. H. Han, T. T. Lin, J. W. Zhou, G. H. Tang and S. Yin, *Chirality*, 2014, **26**, 189–193.

19 T. S. Wu, Y. Y. Chan and Y. L. Leu, *Chem. Pharm. Bull.*, 2000, **48**, 357–361.

20 T. S. Wu, Y. Y. Chan and Y. L. Leu, *J. Nat. Prod.*, 2001, **64**, 71–74.

21 Y. Y. Chan, Y. L. Leu and T. S. Wu, *Tetrahedron Lett.*, 1998, **39**, 8145–8148.

22 Z. B. Cheng, W. W. Shao, Y. N. Liu, Q. Liao, T. T. Lin, X. Y . Shen and S. Yin, *J. Nat. Prod.*, 2013, **76**, 664–671.

23 J. Zhang and L. X. He, *Acta Pharm Sin*., 1986, **21**, 273–278.

24 G. Ruecker, R. Mayer, H. Wiedenfeld, B. S. Chung and A. Guellmann, *Phytochemistry*, 1987, **26**, 1529–1530.

25 T. S. Wu, Y. Y. Chan and Y. L. Leu, *J. Chin. Chem. Soc.*, 2000, **47**, 957–960.

26 C. Y. Ragasa, J. Ganzon, J. Hofilena, B. Tamboong and J. A. Rideout, *Chem.*

Pharm. Bull., 2003, **51**, 1208–1210.

27 C. Gaspar-Marques, M. F. Simoes and B. Rodriguez, *J. Nat. Prod.*, 2004, **67**, 614–621.

28 Z. H. Sun, C. Q. Hu and J. Y. Wang, *Chin. Chem. Lett.*, 2007, **18**, 1379–1382.

29 G. Ruecker, C. W. Ming, R. Mayer, G. Will and A. Guellmann, *Phytochemistry*, 1990, **29**, 983–985.

30 H. Z. Xue, J. Zhang, L. X. He, C. H. He, Q. T. Zheng and R. Feng, *Acta Pharm Sin*.,1989, **24**, 917–922.

31 T. S. Wu, Y. Y. Chan, Y. L. Leu, P. L. Wu, C. Y. Li and Y. Mori, *J. Nat. Prod.*, 1999, **62**, 348–351.

32 T. S. Wu, Y. Y. Chan, Y. L. Leu and Z. T. Chen, *J. Nat. Prod.*, 1999, **62**, 415–418.

33 *Spartan 04*; Wavefunction Inc.:Irvine, CA.

34 *Gaussian 09*, revision C.01; Gaussian, Inc.: Wallingford, CT, 2009. Full list of authors can be found in the SI.

35 P. J. Stephens and N. Harada, *Chirality*, 2010, **22**, 229–233.

Table 1. ^{1}H NMR Data of Compounds 1–6[a]

NO.	1[b]	2[c]	3[b]	4[b]	5[b]	6[b]
1	9.51, s	4.03, dd (8.0, 6.6)	5.84, dd (17.6, 10.8)	5.86, dd (17.6, 10.9)	5.86, dd (17.6, 10.7)	2.01, m
2a		α 1.91, m	5.03, d (17.6)	5.03, dd (17.6, 1.1)	4.99, d (17.6)	1.59, m
2b		β 2.21, m	4.97, d (10.8)	4.95, dd (10.9, 1.1)	4.93, d (10.7)	
3a	7.21, s	α 2.49, m	5.33, s	6.20, s	5.32, s	1.81, m
3b		β 2.59, m	4.97, s	6.19, s	4.94, s	
4						2.55, ddd (15.6, 8.1, 3.0)
5a	5.15, s	2.55, d (5.1)	2.59, s	3.39, s	2.61, s	1.46, m
5b	4.87, s					
6		5.35, dd (5.1, 2.9)				0.51, dd (9.6, 9.6)
7	5.14, dd (7.6, 7.6)	2.35, m	5.61, brs	5.63, dd (3.2, 3.2)	5.55, brs	0.66, ddd (10.6, 9.6, 6.2)
8α	2.23, m	1.53, m	2.09, m	2.07, m	2.06, m	1.85, m
8β		1.82, m				0.94, m
9α	2.10, m	2.31, m	1.64, m	1.38, m	1.30, m	1.57, m
9β		1.10, m	1.38, m	1.34, m	1.62, m	1.73, m
11a	4.85, dd (7.4, 7.4)		2.13, m	2.07, m	2.12, m	
11b			1.87, dd (13.6, 10.0)	1.85, d (14.7)	2.01, m	
12a	2.28, m	4.92, brs	3.86, m	4.96, m	3.89, m	0.98, s
12b						
13a	2.17, m	1.80, s	1.16, d (6.1)	1.15, d (6.2)	1.13, d (5.9)	0.95, s
13b						
14a	1.81, s	1.33, s	4.15, d (14.1)	9.63, s	4.13, d (13.7)	9.54, d (3.0)
14b			4.04, d (14.1)		4.06, d (13.7)	
15	1.44, s		0.93, s	0.72, s	0.90, s	1.11, s
			12-OAc:	1,99, s		

[a]Data were recorded at 400 MHz, chemical shifts are in ppm, coupling constant J is in Hz. [b]In $CDCl_3$. [c]In C_5D_5N.

Table 2. ^{13}C NMR (100 MHz) Data of Compounds 1–6

No.	1[a]	2[b]	3[a]	4[a]	5[a]	6[a]
1	195.6, CH	67.4, CH	146.8, CH	145.5, CH	146.8, CH	57.6, CH
2	144.3, C	26.2, CH_2	111.4, CH_2	111.7, CH_2	111.2, CH_2	26.6, CH_2
3	154.4, CH	27.0, CH_2	114.2, CH_2	137.2, CH_2	114.1, CH_2	26.0, CH_2
4	146.4, C	75.9, C	149.2, C	150.7, C	149.8, C	60.3, CH
5	112.0, CH_2	52.6, CH	49.1, CH	43.3, CH	49.9, CH	39.4, CH
6	132.6, C	79.3, CH	135.3, C	133.2, C	135.7, C	31.8, CH
7	134.8, CH	44.0, CH	125.7, CH	126.1, CH	124.6, CH	27.1, CH
8	24.0, CH_2	19.5, CH_2	22.8, CH_2	22.8, CH_2	22.9, CH_2	20.2, CH_2
9	38.4, CH_2	32.6,CH_2	28.5, CH_2	27.9, CH_2	28.6, CH_2	44.3, CH_2
10	134.2, C	37.0, C	38.5, C	38.3, C	38.6, C	75.1, C
11	126.9, CH	146.2, C	46.1, CH_2	42.1, CH_2	46.8, CH_2	19.7, C
12	24.3, CH_2	111.4, CH_2	64.8, CH	69.1, CH	67.0, CH	28.6, CH_3
13	26.7, CH_2	21.7, CH_3	22.7, CH_3	19.8, CH_3	23.2, CH_3	15.9, CH_3
14	13.9, CH_3	25.0, CH_3	67.6, CH_2	194.1, CH	67.8, CH_2	203.1, CH
15	14.4, CH_3	178.9, C	26.4, CH_3	25.8, CH_3	25.8, CH_3	20.2, CH_3
			–OAc:	21.3, CH_3		
				170.5, C		

[a]In $CDCl_3$. [b]In C_5D_5N

Table 3. IC_{50} Values of the Active Compounds on LPS-induced NO Production in BV-2 Cells

compound	IC_{50}(μM)[a]	compound	IC_{50}(μM)[a]
3	25.0 ± 3.1	**28**	5.7 ± 1.5
4	9.0 ± 1.6	**29**	15.7 ± 2.5
5	29.8 ± 3.2	**30**	8.7 ± 2.2
9	9.9 ± 0.9	quercetin[b]	15.7 ± 2.1
17	19.5 ± 2.7		

[a]Values are represented as means ± SD based on three independent experiments. [b]Positive control.

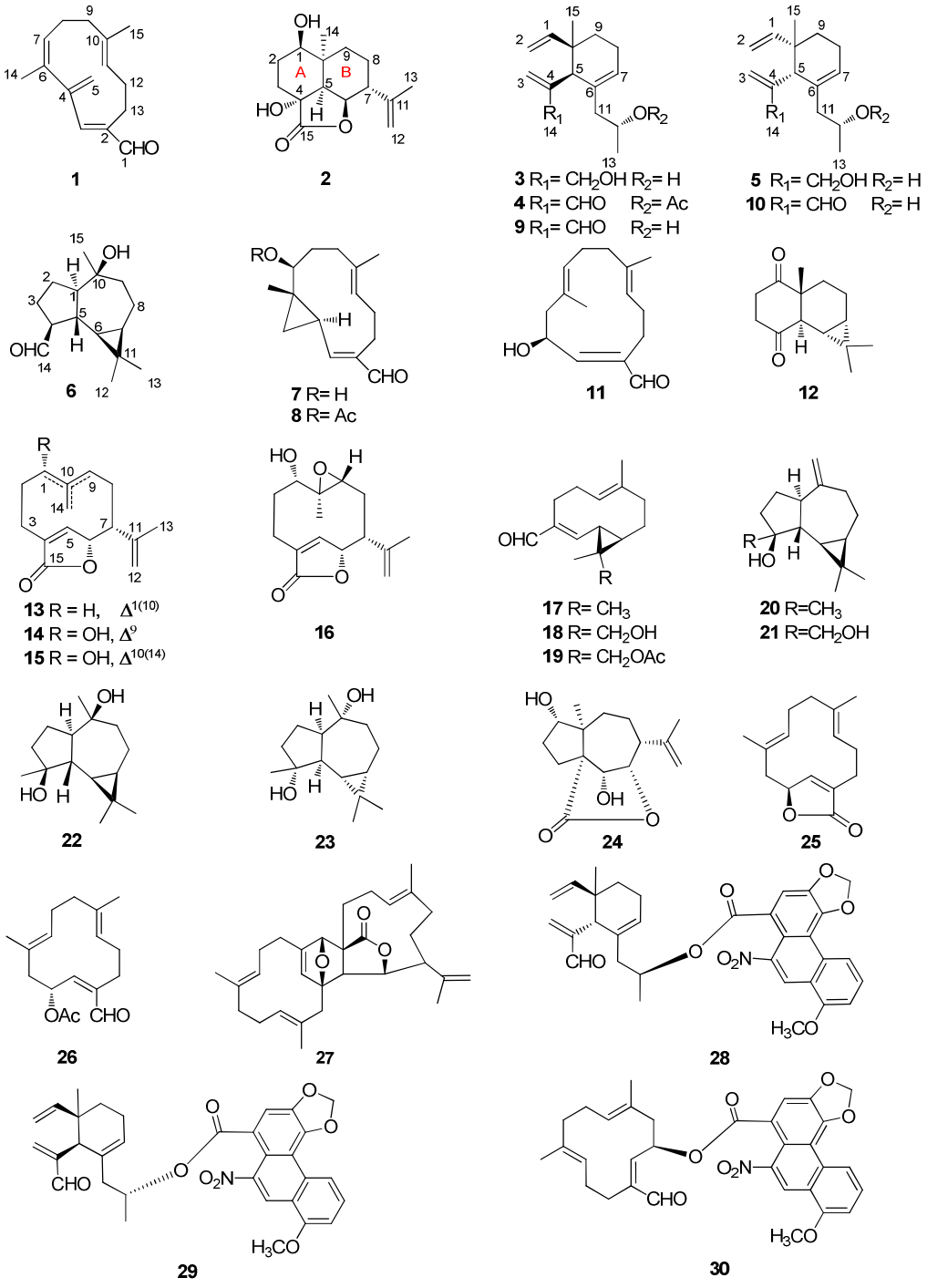

Figure 1. Structures of compounds **1**–**30**.

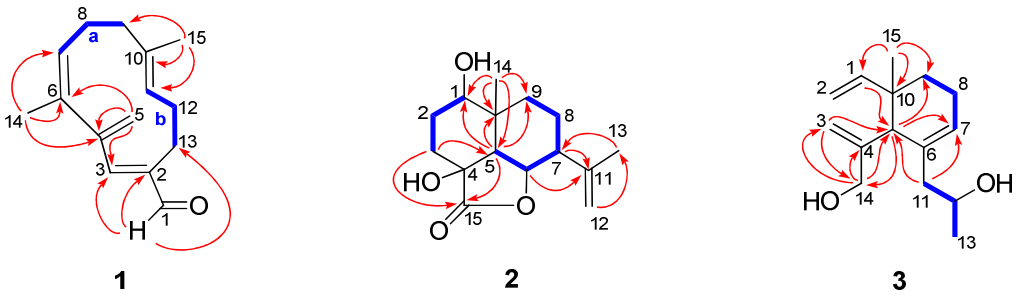

Figure 2. Selected $^{1}H–^{1}H$ COSY (—) and HMBC (→) correlations of **1–3.**

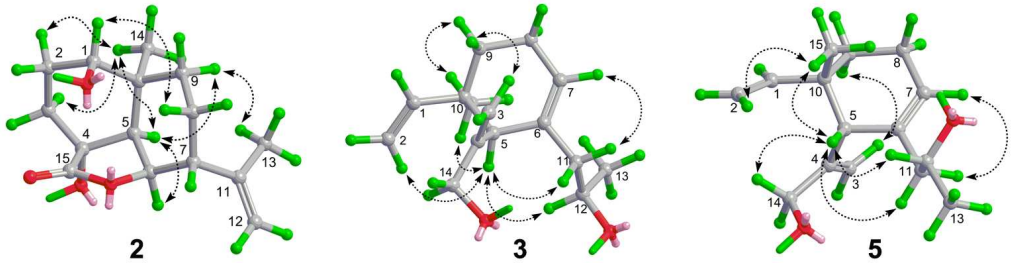

Figure 3. Key NOE correlations (⇢) of **2**, **3**, and **5.**

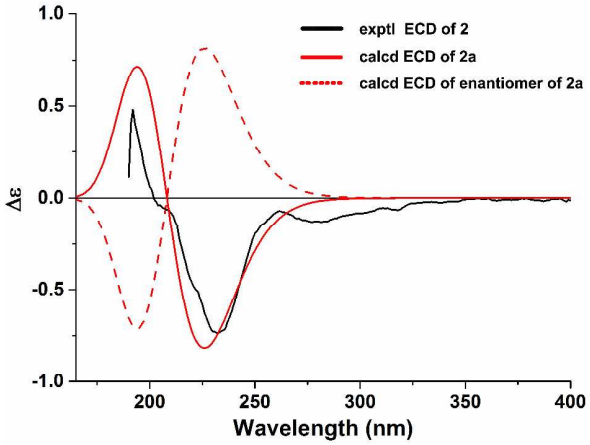

Figure 4. Experimental ECD spectra (190-400 nm) of **2** and TDDFT calculated ECD spectra for **2a** (1*R*, 4*R*, 5*S*, 6*R*, 7*R*, 10*S*) and enantiomer of **2a**

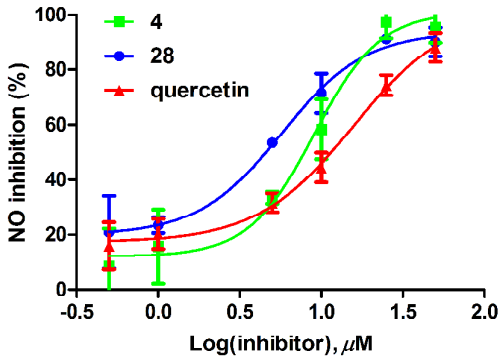

Figure 5. The inhibitory curves of compounds **4**, **28** and quercetin (positive control) on LPS-induced NO Production in BV-2 Cells.

TOC

Six new sesquiterpenoids, including one with a new skeleton, and 24 known analogues were isolated from *Aristolochia mollissima*.